Prospect identification and reservoir characterization using seismic and petrophysical data in 'Famito' field, onshore Niger Delta, Nigeria

Charles Afamefuna Illo[1] · Charles Chibueze Ugbor[1] · Joseph Nanaoweikule Eradiri[1] · Chidubem Okwudiri Emedo[1,2]

Abstract

An integrated seismic and petrophysical study using data from six wells has been carried out across 'Famito' field, Niger Delta Basin. The seismic data was incorporated with porosity and water saturation logs to characterize three hydrocarbon-bearing reservoirs and quantitatively estimate its prospectivity. The reservoirs (F-1000, G-1000, and H-1000) were correlatable across the field with some appreciable reduction in net sand down dip. F-1000 sandstone, the primary reservoir, was partitioned into five different zones (Top 301 to Top 305) to characterize the reservoir properties better. Structural analysis has been carried out using seismic data, which aided the mapping of major, antithetic, and synthetic faults with three horizons (constrained by well log data) that were gridded to create top structural maps. Petrophysical results using well log derived parameters and time-depth structural maps were obtained. Surface attributes, which are highly amplitude supported, were utilized to capture prospective zones better. The study showed that reservoir F-1000 has very good porosity (22–28%), appreciable shale volume (25–33%), and high hydrocarbon saturation (47–90%) with an oil and gas phase. Similarly, G-1000 and H-1000 comprises shaly sands with very good average porosities (25% and 24%, respectively) and high average hydrocarbon saturations (66% and 71%, respectively). Unlike G-1000, which showed an oil and gas phase, H-1000 contains only oil. Surface attribute analysis reveals the existence of hydrocarbon-bearing closures characterized by moderate to high root mean square amplitude and average energy values within G-1000 and H-1000, at the western part of the field. These values are closely consistent with those obtained for F-1000, which hosts the producing wells. Using these methods, this study has unravelled new prospective zones within reservoirs G-1000 and H-1000, allowing for increased hydrocarbon volumes from the already producing oil field.

Keywords Niger Delta · Reservoirs · Surface attributes · Petrophysical parameters · Hydrocarbon

Introduction

Hydrocarbon exploration and development has undergone several step changes in technologies during recent decades, and the integration of seismic and petrophysics workflows is now considered as a robust technique in the effective estimation of the overall reservoir architecture (Aigbedion and

✉ Chidubem Okwudiri Emedo
  Chidubem.emedo.pg.80047@unn.edu.ng;
  ecogeogranite@gmail.com

1 Department of Geology, University of Nigeria,
  Nsukka 410001, Nigeria

2 Department of Geology, Federal University of Technology,
  Owerri 460114, Nigeria

Aigbedion 2011). The value of this integrated technique is recognized worldwide in enhancing accurate reservoir characterization, predicting lithologies, modelling petrophysical properties, and estimating the volume of hydrocarbon-initially-in-place, during the exploration, appraisal, and development phases of a field. As the technology matures, there is an increased emphasis on the quantitative interpretation of reservoir properties, involving well logs and seismic data to estimate variations in both static and dynamic reservoir properties as well as delineate new pay zones. Recently, the significant decline in hydrocarbon reserves across oil-producing nations in Africa, and Nigeria in particular, has become very worrisome (Ugbor et al. 2020). This is because the inability to add to the already depleting hydrocarbon reserve could result in revenue shortages in the near future. With the not-promising results obtained from some frontier basins, there is a need to re-evaluate

reservoirs within relatively older fields for the presence of by-passed hydrocarbon deposits and/or identification of new prospective zones for further consideration. The 'Famito' field in onshore Niger Delta presents a huge opportunity for the delineation of new pay zones. To achieve this, advanced or alternative reservoir characterization techniques that aim to highlight hydrocarbon bearing zones are to be applied. These techniques are capable of improving the reservoir and structural characterization of a field for better prediction of hydrocarbon charged zones.

Several reservoir characterization approaches have been proposed which include the following: (i) characterization of hydrocarbon reservoirs using well log to evaluate hydrocarbon prospects, delineate hydrocarbon and water-bearing zones, and estimate petrophysical properties of the hydrocarbon reservoirs of interest (Horsfall et al. 2015), (ii) prediction of lateral variation in the physical properties of known and potential reservoirs using feedforward neural network by An and Moon (1993), and (iii) mapping of hydrocarbon saturation in relatively unconsolidated sandstone reservoirs using well logs (Eshimokhai and Akhirevbulu 2012). Experience shows that integration of seismic and petrophysics with various surface attributes is important in obtaining qualitative and quantitative estimates of reservoir properties, which in turn reduces uncertainties in delineating prospective hydrocarbon bearing zones. This research focuses on using 3D seismic data and information from five wells, integrated with reservoir and structural evaluation tools for improved understanding of the structural configuration, stratigraphic framework, and reservoir architecture and framework. Emphasis was placed on the use of surface attributes for reservoir characterization. Also, fault mapping, identification of hydrocarbon trapping mechanisms, reservoir parameters estimation, and generation of depth and time top structural maps for prospects identification were carried out. For the first time, we have applied three distinct surface/horizon attributes in identifying new prospective zones which have not been drilled previously. A review of past literature shows that the root mean square amplitude and average energy surface attributes are yet to be applied in hydrocarbon prospective studies in the 'Famito' field, Niger Delta, which is located within the Coastal Swamp Depobelt, Niger Delta Basin, and lies within the Gulf of Guinea situated in the West African margin.

This study, therefore, presents a modified interpretation scheme where seismic and well log data are integrated. The results show new prospects of potential hydrocarbon pockets as seen in time structural maps with good reservoir properties estimated from well log data.

Regional geologic framework

The study area, 'Famito' field, discovered in 1958, is situated in the Coastal Swamp Depobelt of the Niger Delta area and belongs to Shell Petroleum Development Company (SPDC) concession (Fig. 1a–c). The field is located in the swampiest of the ecological zones and consists of a massive swamp, dotted with islands of dry land covering about 10,240 square kilometres (Unukogbon et al. 2008). The tectonic framework of the continental margin along the West Coast of equatorial Africa is controlled by Cretaceous fracture zones expressed as trenches and ridges in the deep Atlantic (Omatsola 1989; Tuttle et al. 1999; Weiner et al. 2010). The fracture zone ridges subdivide the margin into individual basins and, in Nigeria, form the boundary faults of the Cretaceous Benue-Abakaliki Trough, which cuts far into the West African shield (Evamy et al. 1978; Reijers 2011). The trough represents a failed arm of a rift triple junction associated with the opening of the South Atlantic. In this region, rifting started in the Late Jurassic and persisted into the Middle Cretaceous (Lehner and De Ruiter 1977; Pochat et al. 2004; Weiner et al. 2010; Dim et al. 2018). In the region of the Niger Delta, rifting diminished altogether in the Late Cretaceous and gravity tectonism became the primary deformational process (Fig. 1).

The Niger Delta Basin structures and stratigraphy have been controlled by pre- and syn-sedimentary tectonics related to the interplay between rates of sediment supply and subsidence as described in Knox and Omatsola (1989) and Stacher (1995). The structural zones according to Corredor et al. (2005) included the extensional province on the shelf, the mud diapirs province, the detachment fold province, the inner fold and thrust belt, the translational province, and the outer fold and thrust belt in the deepwater end (Fig. 1d). The Niger Delta stratigraphic sequence comprises an overall regressive association of Cenozoic (Eocene to Recent) clastics (up to 12,000-m thick), formed by three diachronous lithostratigraphic units (Cant 1992; Selley 1998; Klett et al. 1997; Ehinola et al. 2010) (Fig. 2). They include marine claystones and shales of the Akata Formation; alternation of sandstones, siltstones, and claystones of the paralic Agbada Formation; and continental alluvial sands and clays of the Benin Formation (Whiteman, 1982; Doust and Omatsola, 1990). The sands of the Agbada Formation, which are Eocene to Holocene in age, constitute the hydrocarbon reservoirs in the Niger Delta Basin.

The most common hydrocarbon trapping mechanism in the Niger Delta consists of roll-over anticlines, collapsed growth fault crests, or in steeply dipping flank faults that result in a juxtaposition of shale units against reservoir
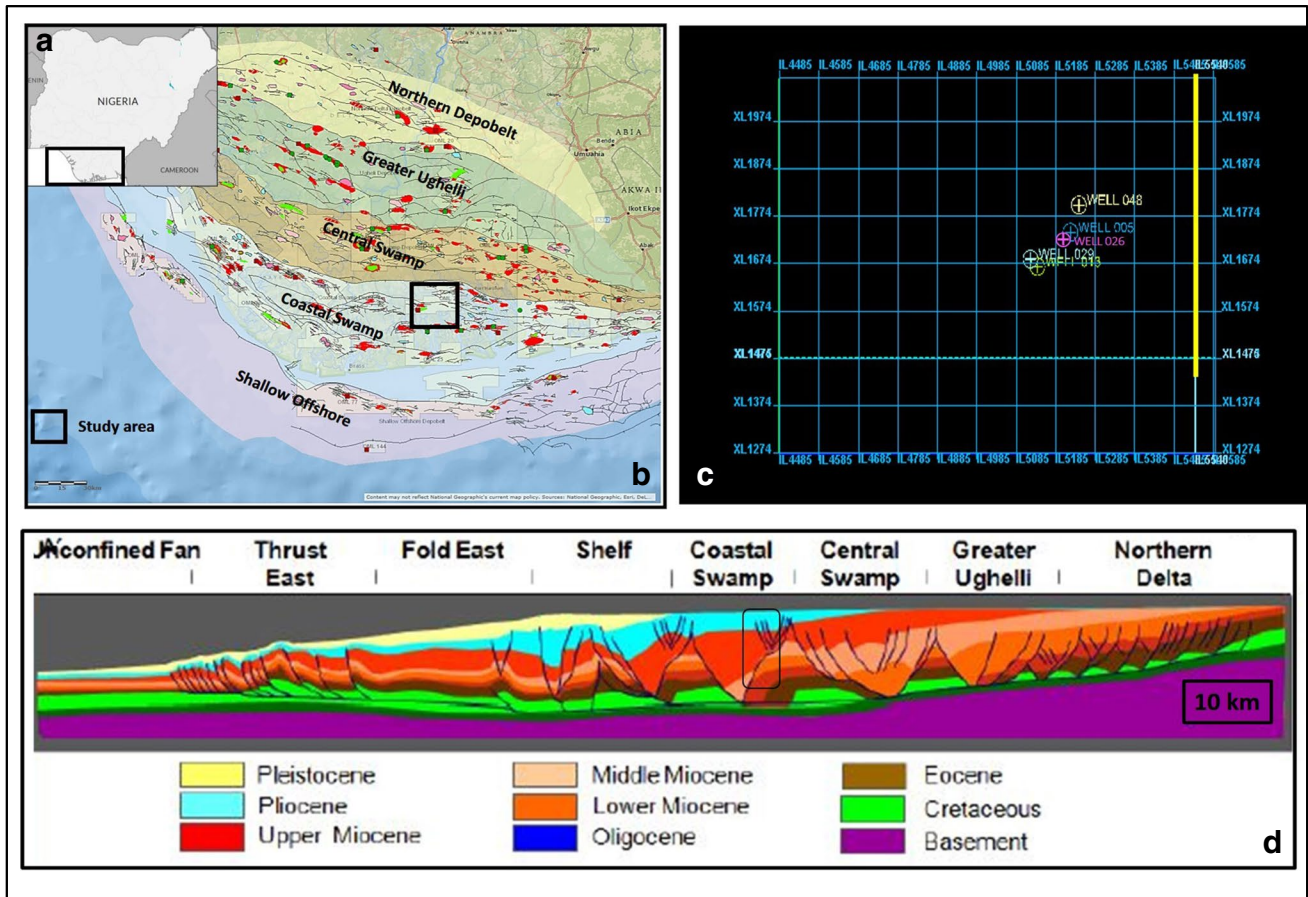
Fig. 1 **a** Map showing Nigeria with location of the Niger Delta Basin (modified after Alao et al. 2013). (**b**) Map of the oil fields within depobelts. (**c**) Seismic survey base map with well locations. (**d**) Regional structural cross section of the Niger Delta Basin (redrawn after Doust and Omatsola 1990)

sandstone units (Doust and Omatsola, 1990; Ehinola and Ejeh 2009; Aigbedion and Aigbedion 2011; Dim et al. 2018). Stratigraphic traps have however become more significant outboard of the shelf, where turbiditic channel and lobe sands are encased in deep marine shales.

Data and method

The dataset used for this study includes three-dimensional seismic data, a suite of well logs from five wells (005, 013, 026, 029, and 048), which penetrated the target reservoirs, check-shot data from three wells, and biostratigraphic data from two wells. The data was integrated and analysed using Schlumberger's Petrel™ software. The complete suite of composite well logs includes gamma ray (GR), resistivity (LLD), compressional sonic (DT), density (RHOB), neutron (CNL), and calliper logs.

A general quality check was carried out on the seismic data and well logs. The seismic volume was checked

to examine the clarity of the volume, the vintage type, the record length, and the survey area covered. The wells were also suitably examined to remove high-frequency occurrences on the well logs and also to check if there are zones of washout and rugosity using the calliper log. Well to seismic tie was carried out to represent the intervals interpreted on the seismic data with those same markers penetrated in the well, with a high level of accuracy. Top of potential reservoir zones were interpreted on the well log and a field-wide correlation was carried out along the dip direction (N-S). Facies, depositional environments, and stacking patterns were interpreted from observed well log motifs, as shown in Cant (1992) and Selley (1998). Seismic interpretation was conducted which involved mapping top reservoir horizons and faults across the seismic volume. Seismic attribute maps (root mean square amplitude, maximum amplitude, and average energy) were also generated to further indicate bright spots, which predict hydrocarbon presence. Velocity model was generated using the sonic log, which facilitates the conversion of picked events and structures from time to depth.
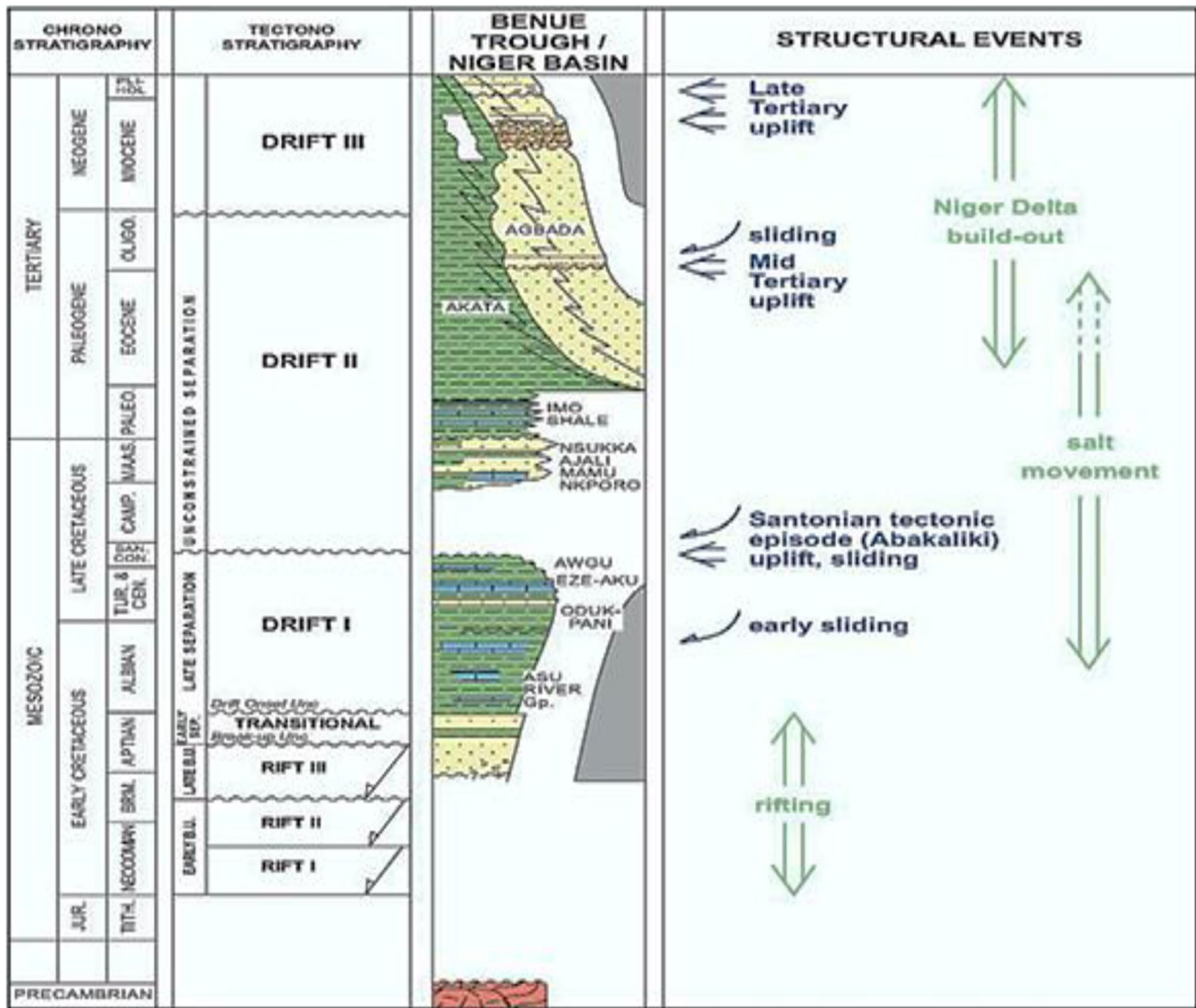
Fig. 2 Study area stratigraphy (adapted from Steve et al. 2002)

Estimation of the petrophysical parameters (net to gross, shale volume, porosity, water saturation, and hydrocarbon saturation) was carried out using Interactive Petrophysics® software. The equations (Eqs. (1–6)) used in the estimation of these parameters are briefly described below:

Shale volume (Vsh)

The gamma ray log was used to compute the volume of shale in the reservoir. As an initial step, the gamma ray index was calculated using the equation below (Glover 2013):

$$I\text{GR} = \frac{GR_{\log} - GR_{\min}}{GR_{\max} - GR_{\min}} \tag{1}$$

where IGR is the gamma ray index, $GR_{\log}$ the gamma ray reading, $GR_{\min}$ the minimum gamma ray (clean sand), and $GR_{\max}$ the maximum gamma ray (shale).

After obtaining the gamma ray index, the volume of shale was calculated by using the Larimov equation for tertiary unconsolidated deposits (Glover 2013).

$$V_{sh} = 0.083 \left[2^{3.7 \times 1GR} - 1.0 \right] \tag{2}$$

Porosity (ϕ)

Porosity, which is the percentage of pore spaces to the total volume of the rock, was determined from density log using the equation of Asquith and Krygowski (2004).

$$\Phi D = \frac{p_{ma} - p_b}{p_{ma} - p_{fl}} \tag{3}$$

where p_{ma} is the matrix density (usually 2.65 g/cc sandstone), p_{fl} the formation fluid's density (1.0 gm/cc for water and 0.8 g/cc for hydrocarbon), p_b the formation bulk density (obtained from density log at 0.5 ft. interval), and p_{sh} the density of adjacent shale body.

Permeability (K)

The ability of a reservoir to transmit fluids is commonly expressed by its permeability. This property is controlled by the size of its connecting pore throats. The relation below was used to obtain permeability values for the target reservoir (Opara 2010).

$$K = \frac{8581 * \Phi_e^{4.4}}{Swirr^2} \tag{4}$$

where K is the permeability in millidarcies, Φ the porosity, S_{wirr} the irreducible water saturation.

Water saturation (Sw)

Water saturation of the target reservoir was determined using the Simandoux equation (Amigun and Bakare 2013).

$$\frac{1}{R_t} = \frac{\Phi_e^m * S_w^n}{a * R_w} + \frac{Vsh * S_w}{R_{sh}} \tag{5}$$

where V_{sh} is the volume of shale, Φe the effective porosity, S_w the water saturation of the uninvaded zone, R_t the true formation resistivity, R_w the resistivity of formation water, R_{sh} the resistivity of shale, n the saturation exponent, m the cementation factor, and a the tortuosity factor.

Hydrocarbon saturation (Shc)

The expression below was used to estimate the hydrocarbon saturation of the reservoir (Anene et al. 2018).

$$S_h = (1 - S_w) \tag{6}$$

Results

Well to seismic tie

The calibration step involving the generation of a synthetic seismic from the well data and comparing it to the actual seismic data collected over the area is an important basis for any integrated study involving seismic and well data. For this study, this step was carried out using the check-shot data calibrated to the sonic log. The wavelet extraction window was displayed to get the extracted wavelet and for the bulk shifting for an accurate tie. Bulk shifting was done within the area of interest at a rate of 35 ms. A synthetic seismogram trace was generated by the convolution of acoustic impedance (density and sonic log) and the extracted seismic wavelet. Three reservoir tops (F-1000, G-1000, and H-1000) were delineated and mapped on the seismic data (Fig. 3). The result shows that these reservoirs are gradually dipping reflectors that form part of the limb of a gently folded anticlinal structure. The yellow arrows represent a trough-polarity, which indicates the seismic wavelet's minimum (negative) deflection, signifying the top of reservoirs. The red arrows show that reflections were pulled up in time to achieve an accurate tie.

Structural (fault) interpretation

Fault picking was done on the seismic volume to show the structural pattern of the field. Faults were interpreted and assigned on every tenth inline, except in areas towards the field's southern part associated with tuning effects. Ten major faults were interpreted. The faults have a curved face in plain few, mostly trend in a dominantly E-W direction, and dip to the south (Fig. 4). The area is intensely faulted with small-scale faults that are hardly detected on cross sections and are not bounded on conventional 3D seismic amplitude (semblance) time slices. The faulting has been interpreted as syn-sedimentary deformation, resulting from the load of the overlying sediments. In particular, closely spaced listric faults southwards of the study area form gently dipping, broad flexures. Several faults in the study area exhibit examples of fault relay and transfer zones previously described in extensional settings (Peacock et al. 2000).

Stratigraphic (horizon) interpretation

The stratigraphic interpretation was carried out to produce top structural maps of key sandstone reservoirs. Three key reservoir horizons, namely, F-1000, G-1000, and H-1000, were identified and interpreted (see Fig. 3); they are guided by the seeded 2D autotracking and manual method across the seismic volume generally showing medium amplitude and laterally continuous reflections. After the horizon mapping, time structure maps of the three horizons were generated which showed evolution in the topographic highs and lows in the basin, linked to interplay of tectonics and rates of sediment supply.

Depth conversion

The time structure maps (Fig. 5a–c) for the three horizons of interest were converted to depth structure maps (Fig. 5d–e)
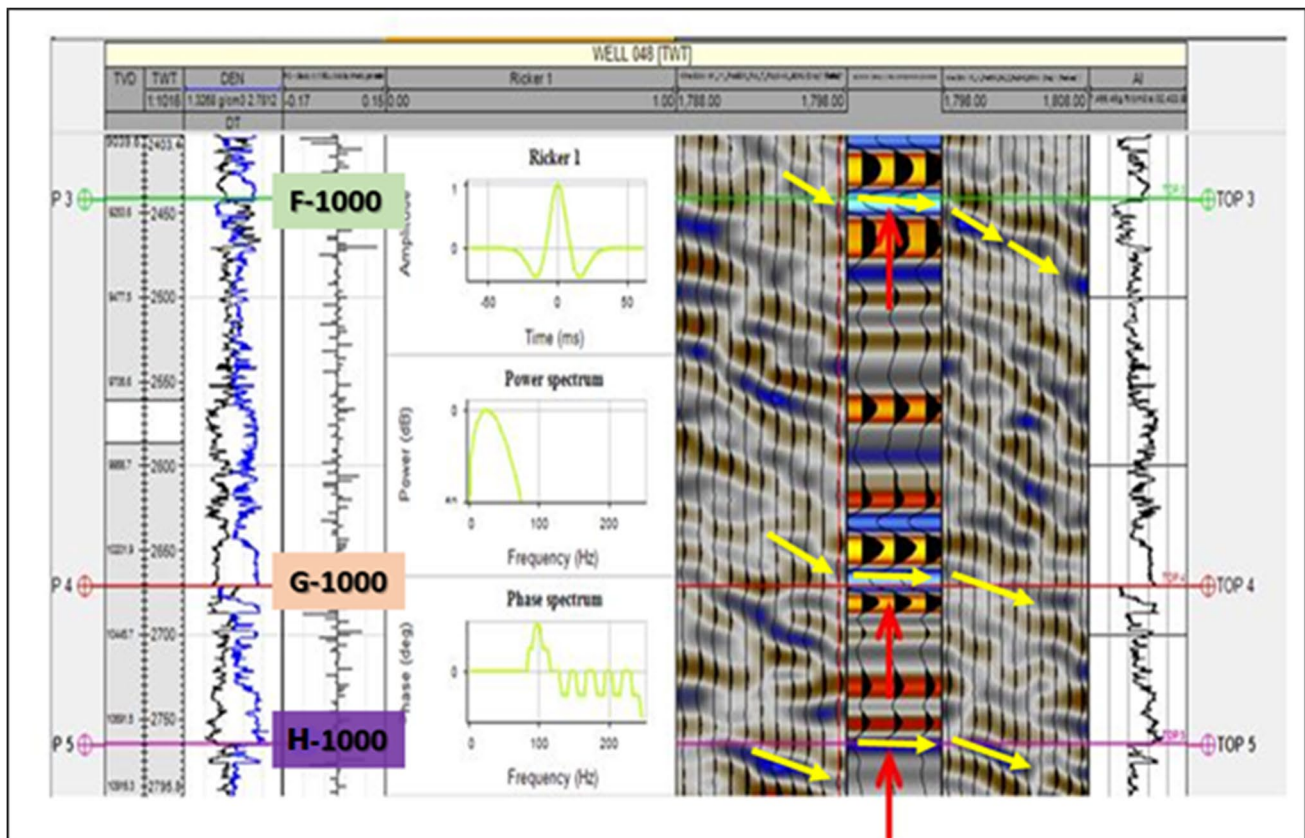
Fig. 3 A sample of well to seismic tie based on the generation of synthetic seismogram for F-1000, G-1000, and H-1000 reservoirs in well-048

using the velocity model, which enabled the integration of the seismic interpretation with well log and petrophysical interpretation. The direct method of time-depth conversion using a third-order polynomial was adopted in this study. With this method, a polynomial equation was derived from the check-shot data of well-048 by cross-plotting depth versus time to obtain a time-depth relationship (TDR). The resultant third-order polynomial function (Eq. 7) was then applied in the depth conversion.

$$y = 6 \times 10^{-11}x^3 + 0.004x^2 + 2.8163x - 23.613 \tag{7}$$

From the displayed time structural contour maps, which were created from the three mapped horizons in the seismic section, F-1000, G-1000, and H-1000, it shows that the geological formation possesses different features such as upfolded, down-folded, dipped gently, and dipped steeply in different parts of the field. A completely round contour closure signifies an upfolded subsurface. The top of the feature is seen by the smallest inward closure. Hydrocarbon accumulation may be present in such areas. One major anticline (labelled A) and two minor anticlines (labelled B and C) are seen in three different parts of the field as the major closures (Fig. 5). Wells drilled in this field are all situated around

the anticline labelled A which validates the interpretation of possible hydrocarbon presence. The anticlines B and C, represented towards the field's west flank, show alternating up-fold and down-fold subsurface structures. The steeply dipping portion of the sedimentary bed shown by closely spaced group of contours decreasing towards the same west flank part of the map predicts a prospective area because hydrocarbon can be seen to occur in the high area. These steeply dipping features may indicate faulted part of the formation, tilted lithofacies, or an unconformable surface. To minimize high risk and cost of drilling and encourage production optimization, exploratory wells could be drilled first on anticline B to test the predicted stratigraphy for oil and gas accumulation. Anticline C is not fully amplitude supported referring to the colour legend. This stipulated closure can be because of high net to gross or possibly hydrocarbon compartments of low economic quantity.

The maps generated revealed one major growth fault trending the NW flank of the field (Fig. 5). Several antithetic and synthetic minor faults, represented with varying lengths, were seen to be distributed at different locations in the western part of the field (Fig. 5). Growth faults and anticlines are apparent in this field and could serve as hydrocarbon traps. Anticlines and fault-assisted closures are good hydrocarbon
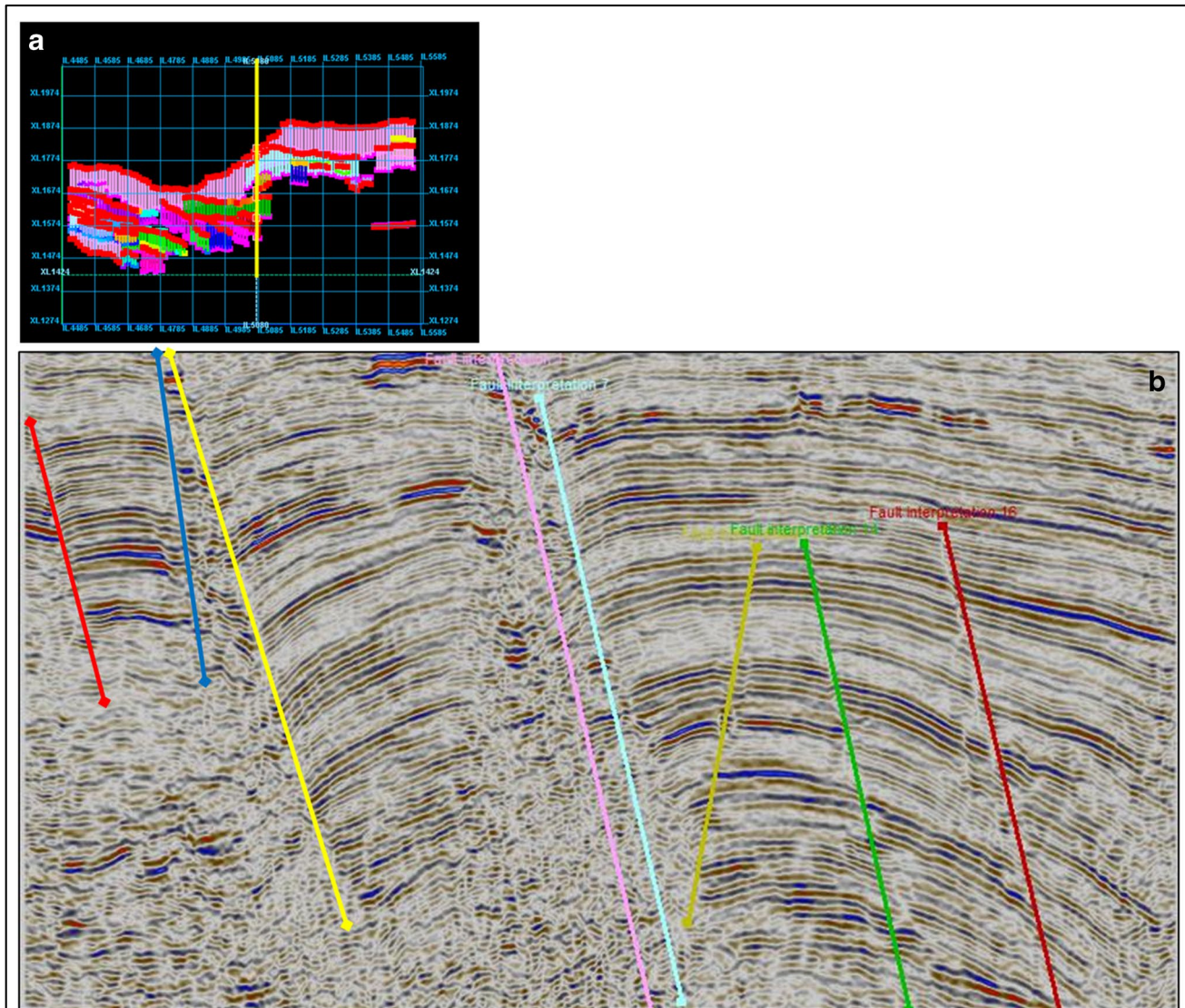
Fig. 4 **a** and **b** are faults picked on 3D seismic volume

prospects in the Niger Delta (Weber and Daukoru 1975; Alao et al. 2013).

Well log facies analysis and correlation

A lithologic correlation was done across five out of the six wells located along the depositional dip (N-S) direction, based on observed well log motif. Sand development was evident towards the southern part of the field (Fig. 6a). The reservoirs of interest (F-1000, G-1000, and H-1000 sands) were delineated and an intra-reservoir correlation was done using the F-1000 reservoir to show the stacking pattern and lithological variation across the wells (Fig. 6b).

Five intra-reservoir markers were correlated across the field and show good sand development towards the southern part of the F-1000 reservoir, most likely controlled by

syn-depositional growth faulting (Fig. 6b). Three stacking patterns were recognized, which include progradation, retrogradation, and aggradation patterns. The progradational (fore-stepping) stacking patterns were recognized as gradual upward decreasing gamma ray values. During this period, accommodation space was filled more rapidly than created, and facies progressively moved farther seawards over time, building to form coarsening upward sequences (Catuneanu et al. 2011). The retrogradational (back-stepping) stacking patterns are recognized as a gradual upward increase in gamma ray value, which indicates a fining upward sequence. Here, there was more accommodation (water depth becomes deeper) than there is fluvial input, and facies moved farther landwards. Aggradational stacking patterns had no net shift in gamma ray log value. It was interpreted as episodes where water depths remain constant from on parasequence to

Fig. 5 **a**, **b**, and **c** Time structural maps of the reservoirs. **d**, **e**, and **f** Depth structural maps of the reservoirs
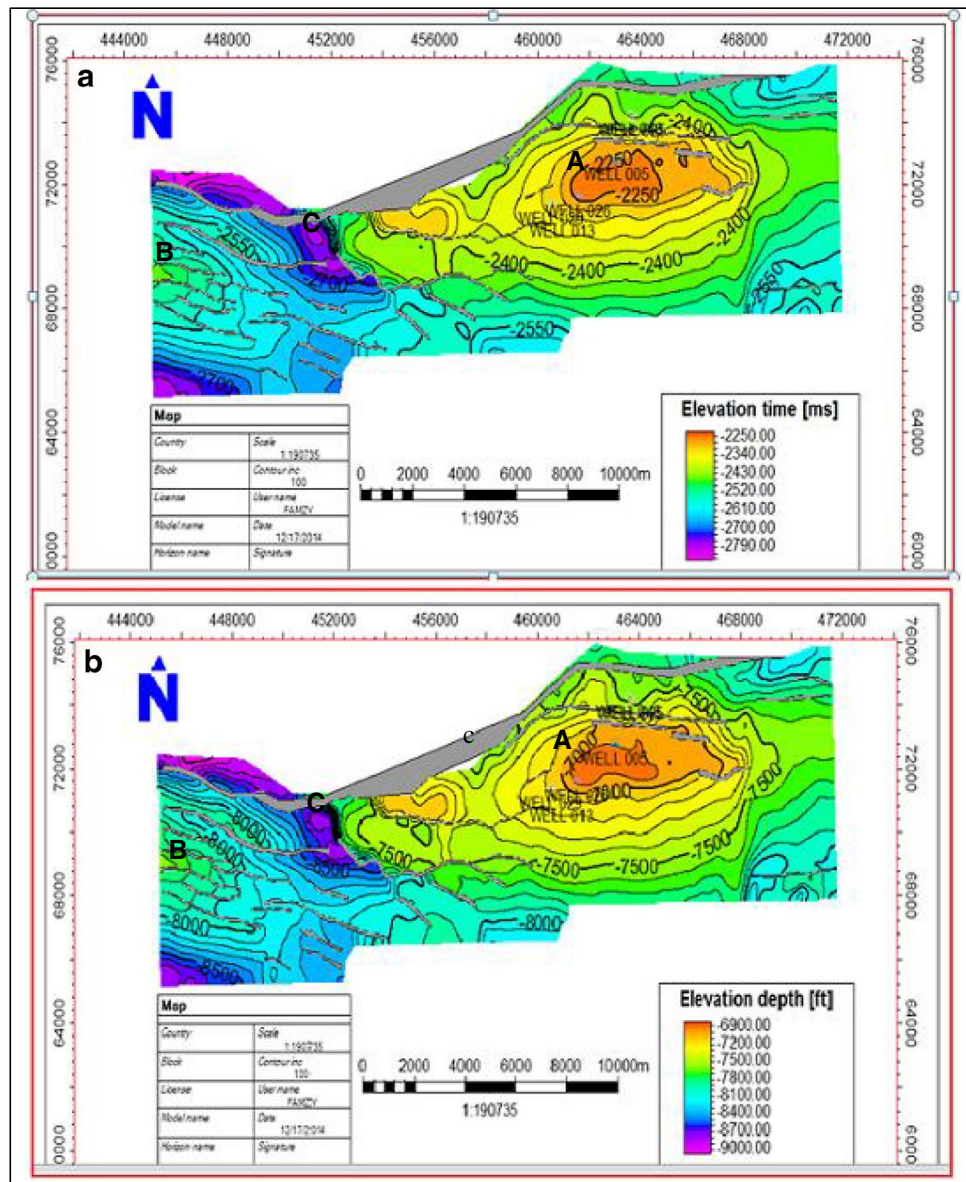
the next and facies show no net landward or seaward movement (Catuneanu et al. 2011). Overall, the reservoir facies interpreted from log motifs are fluvial/tidal distributary channels with blocky profiles and serrated log signatures, respectively, while shoreface sands were mostly prograding and coarsening upwards.

Petrophysical evaluation

Important petrophysical parameters (net to gross, shale volume, porosity, water saturation, and hydrocarbon saturation) were estimated for the key reservoirs in the 'Famito' field. Using gamma ray and resistivity logs, potential hydrocarbon intervals (clean sand with high resistivity) were identified. Porosity interpretation carried out in this study was done

using the density porosity calculation. The formation density and neutron logs were used for the differentiation of the various fluid types. The gas zones are interpreted from the crossover of the formation density and neutron logs, oil zones are based on high resistivity values, and water zones correspond to very low resistive areas.

Five zones (Top 301, Top 302, Top 303, Top 304, and Top 305) including the thin intra-zone shale layers were delineated for reservoir F-1000 (Fig. 7a). The volume of shale ranges laterally across the field from 25% (in well-005) to 33% (in well-029), porosity values range from 22% (in well-029) to 28% (in well-048), while hydrocarbon saturation ranges from 47% (in well-048) to 90% (in well-026). For G-1000 reservoir (Fig. 7b), shale volume

Fig. 5 (continued)
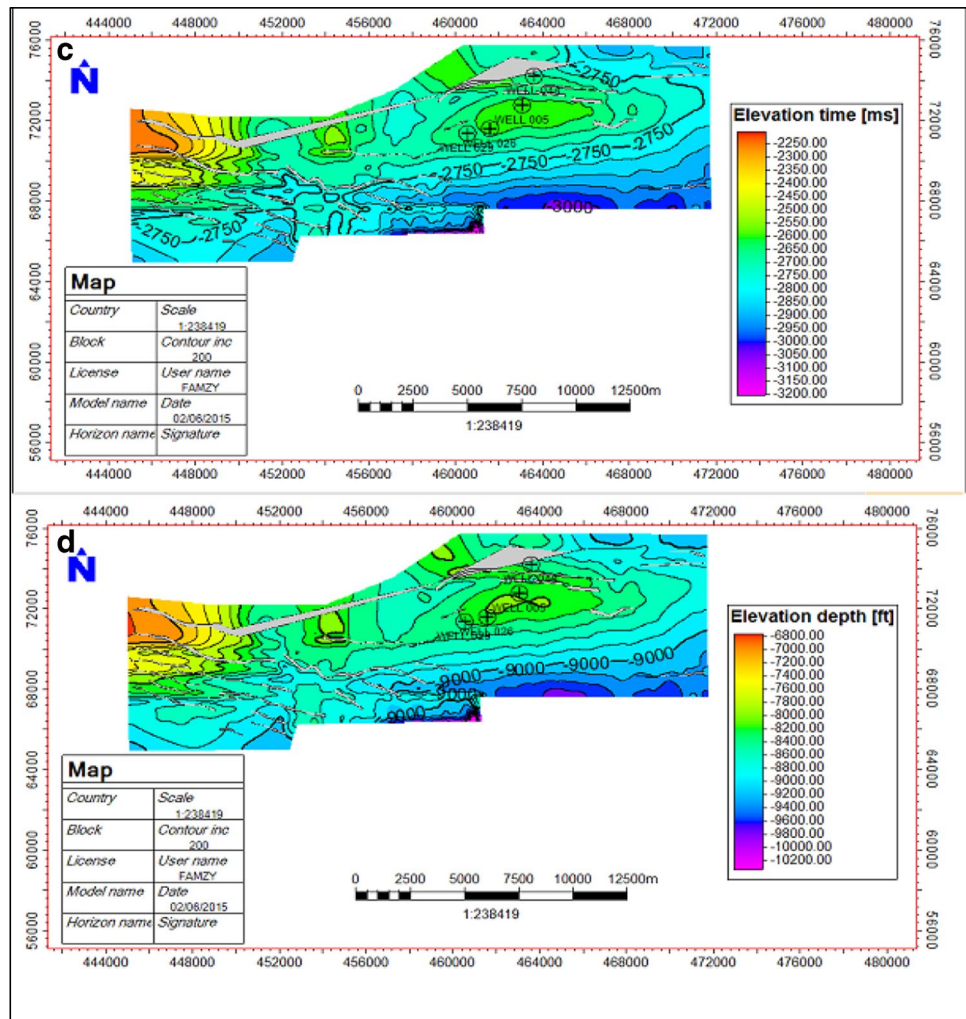
ranges from 0.16% (in well-029) to 0.23% (in well-048), porosity ranges from 21% (in well-005) to 31% (in well-048), while hydrocarbon saturation ranges from 56% (in well-048) to 72% (in well-005). Furthermore, reservoir H-1000 (Fig. 7c) shale volume ranges from 19% (in well-026) to 41% (in well-029), porosity ranges from 22% (in well-026) to 28% (in well-048), while hydrocarbon saturation ranges from 62% (in well-048) to 82% (in well-026). A summary of average estimated petrophysical properties per well for reservoirs F-1000, G-1000 (with two zones — Top 401 and 402), and H-1000 (with three zones — Top 501, Top 502, and Top 503) is shown in Table 1. These parameters, especially porosity and permeability, enabled the lateral distinction of subzones and units within the reservoir which correspond to areas of similar flow behaviour that could serve as high prospective zones for hydrocarbon production or water injection for oil recovery (Nabawy and Sharawy 2015; El Sharawy and Nabawy 2016; Radwan et al. 2021).

Surface attribute analysis

Attributes enable clear identification and delineation of structural and stratigraphic elements that can be interactively calculated directly from maps. The main objectives of surface attributes are, first, to correctly image the structure in time and depth and second, to characterize amplitudes of the reflections.

From the three delineated reservoirs, surface attributes such as root mean square (RMS) amplitude, maximum amplitude, and average energy, which serve as good measure for hydrocarbon prospects, were generated to capture the subsurface structure and possibly identify new pay zones. The results from the interpretation indicate that hydrocarbon presence is close to the strong amplitude on these extracted attribute maps. One major closure was identified from the attribute maps for F-1000 reservoir (Fig. 8), which is bounded by growth fault and some antithetic minor faults. This closure is seen to be amplitude supported, revealing a bright spot zone. All the producing wells drilled in this

Fig. 5 (continued)
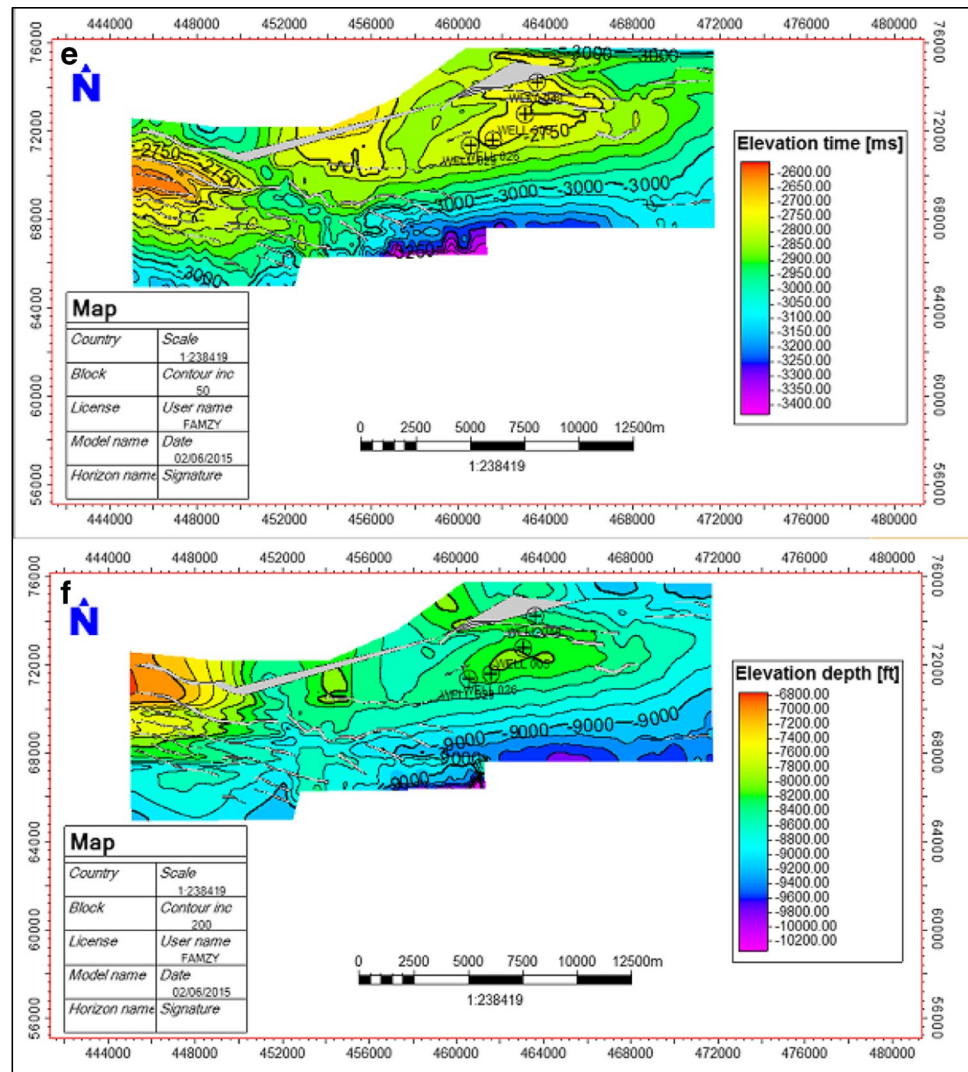
field are within the specified closure, indicating a hydrocarbon charged zone. This provides a good guide for enhanced assessment of the overall reservoir structure and more prospective optimization of infill-well locations and completion for increased reserve. For the RMS amplitude attribute map (Fig. 8a), the amplitude ranges from 2800 to 7000, showing moderate to high values anomaly, predicting hydrocarbon existence. The maximum amplitude attribute map (Fig. 8b) showed high amplitude values ranging from 5000 to 9000, revealing how amplitude supported the identified zone is, thus giving additional confidence for enhanced producibility. The average energy attribute map (Fig. 8c) shows low to medium values ranging from 1000 to 4000. F-1000 reservoir shows just one zone of interest, which is situated at the north-eastern part of the field. There is no other clear evidence of hydrocarbon presence in other parts of the field.

This interpretational procedure on surface attribute amplitude maps for F-1000 reservoir holds also for G-1000 and H-1000 reservoirs. In the G-1000 reservoir, one closure

is seen, which is highly amplitude supported. The RMS amplitude attribute map (Fig. 9a) demonstrated a moderate amplitude range of 4000 to 7500. The high range amplitude values were seen on the maximum amplitude attribute map (Fig. 9b), ranging from 5000 to 9500. Average energy values range from 3000 to 6500 (Fig. 9c). H-1000 reservoir exhibits amplitude supported range of values for RMS, maximum amplitude, and average energy to be 3500–5500, 4000–7500, and 18,000,000–45,000,000, respectively (Fig. 10a–c). G-1000 and H-1000 reservoirs have structures away from the main closure that is amplitude supported.

Discussion

The well logs and petrophysical parameters from this study suggest that lithology discrimination between sand and shale, and petrophysical evaluations for porosity, volume of shale, net to gross, and water and hydrocarbon saturations
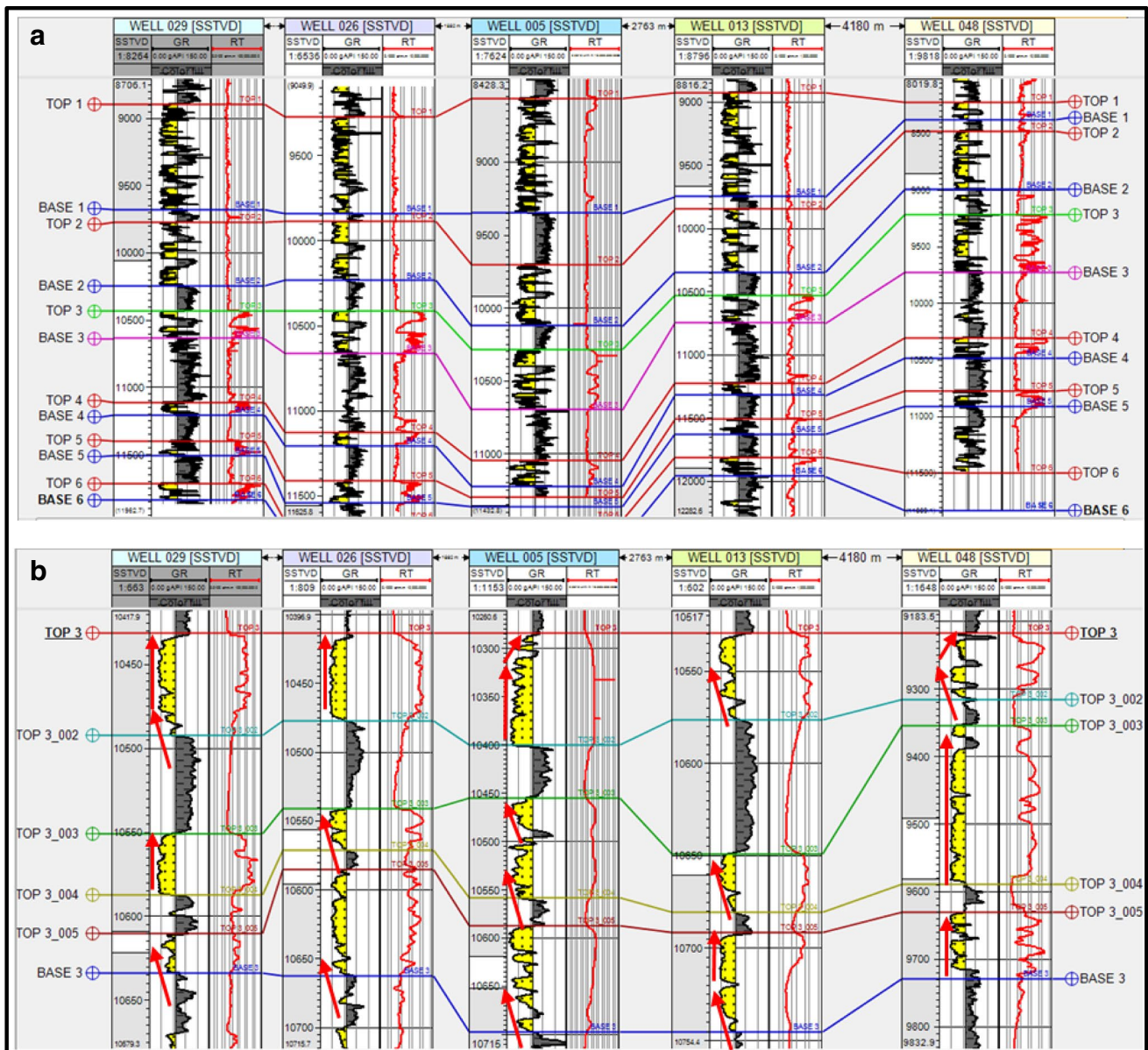
Fig. 6 a Lithostratigraphic interpretation of the reservoirs. **b** Stacking pattern showing the facies arrangement (correlation flattened at top of H-1000)

are probable. Sand production was more evident basinwards for reservoir F-1000. This could be linked to syn-depositional faulting. The gamma ray logs and the high porosity sandstone facies showed a clear association. The hydrocarbon-saturated sand zones in the studied formation often correspond to the high resistivity values in the petrophysical reservoir model. From the petrophysical analysis chart, when comparing the thickness of the F-1000 reservoir to reservoir thicknesses of G-1000 and H-1000 across the wells, the F-1000 reservoir showed a higher thickness of about 338 ft on average with good porosity (Table 1). As a result, the F-1000 reservoir possesses more hydrocarbon storage

space and perhaps better pore connectivity for fluid flow. In well-029, F-1000 and H-1000 reservoirs show higher shale volumes when compared with G-1000 reservoir. The major difference in reservoir quality as regards clear variation in this petrophysical property across the stipulated well is associated with the degree of sorting of sandstone, which is fundamentally controlled by depositional environments and processes as well as the amount of shale present in each reservoir unit (Saadu and Nwankwo 2018).

Figure 4 is a detailed example of the structural distribution within the field. The generally closed spaced listric faults southwards of the study area that form gently dipping
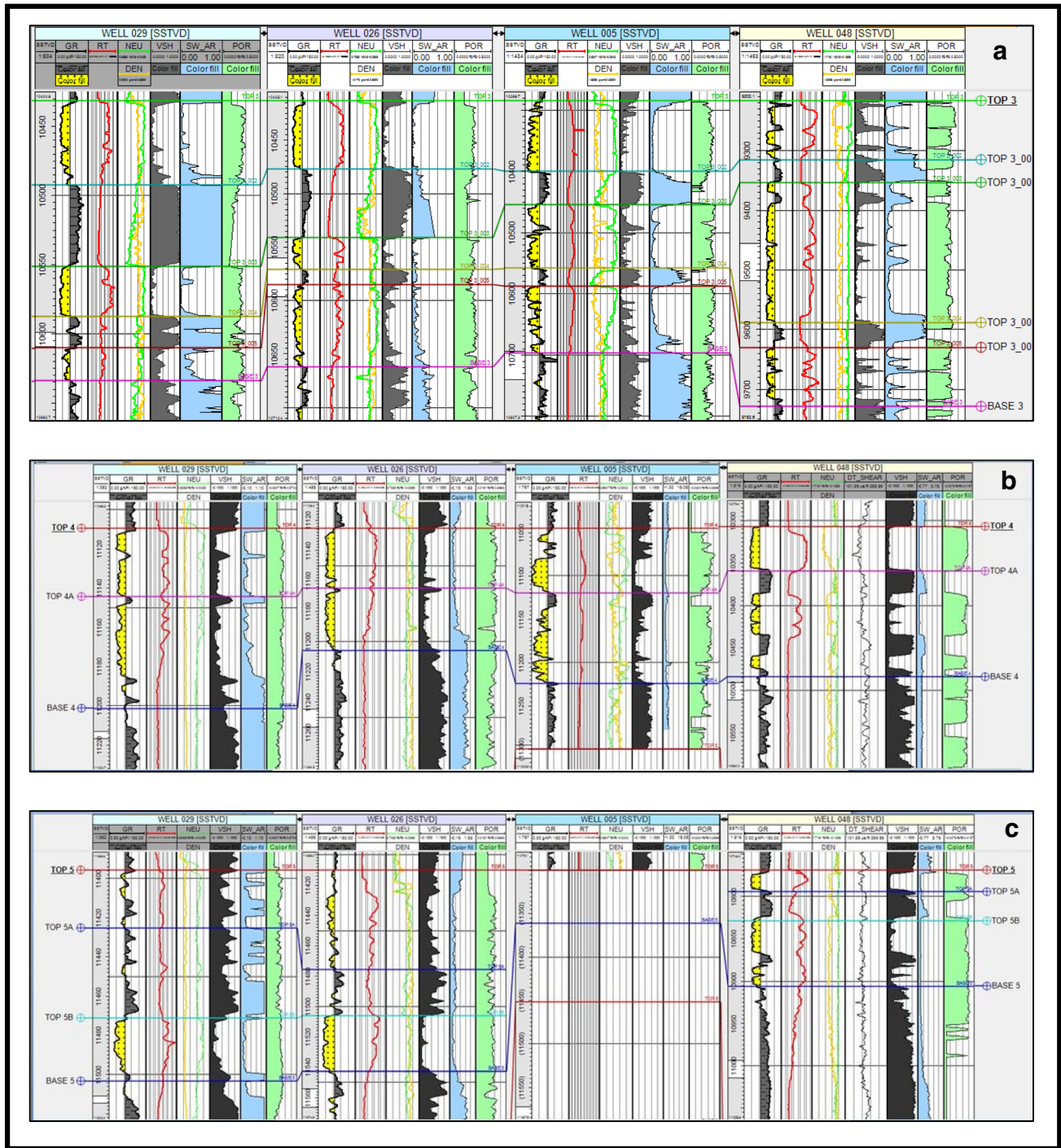
Fig. 7 Petrophysical interpretation of **a** F-1000, **b** G-1000, and **c** H-1000 reservoirs

broad flexures suggest fault relay and transfer zones, which was previously described in extensional settings (Peacock et al. 2000). In addition, the steeply dipping portion of the sedimentary bed shown by closely spaced group of contours decreasing towards the same west flank part of the map predicts a prospective area because hydrocarbon can be seen to occur in the high area. These steeply dipping features may

indicate faulted part of the formation, tilted lithofacies, or an unconformable surface. To minimize high risk and cost of drilling and encourage production optimization, exploratory wells could be drilled first on anticline B (Fig. 5a–b) to test the predicted stratigraphy for oil and gas accumulation. Anticline C is not fully amplitude supported as shown in the colour legend. This could be attributed to high net to

Table 1 Petrophysical analysis chart of F-1000, G-1000, and H-1000 reservoirs

| Reservoir names	Wells (SSTVD)	Net to gross (v/v)	V_{SH} (v/v)	ϕ (v/v)	S_W (v/v)	S_H (v/v)	Fluid type	Pay thickness (ft)	Depth (ft)
F-1000	Well-005	0.6850	0.2450	0.2243	0.4573	0.5427	Predicted gas zone	400	10,300
	Well-026	0.6337	0.3105	0.2365	0.1064	0.8936	Predicted gas zone	250	11,400
	Well-029	0.6125	0.3275	0.2197	0.4510	0.5490	Predicted gas zone	200	10,425
	Well-048	0.6900	0.2650	0.2799	0.5315	0.4685	Predicted oil zone	500	9250
G-1000	Well-005	0.6944	0.2040	0.2087	0.2754	0.7246	Predicted gas zone	200	11,050
	Well-026	0.7955	0.1707	0.2408	0.3270	0.6730	Predicted oil zone	75	11,125
	Well-029	0.7526	0.1610	0.2512	0.3234	0.6766	Predicted oil zone	75	11,125
	Well-048	0.6667	0.2348	0.3102	0.4444	0.5556	Predicted oil zone	200	10,300
H-1000	Well-026	0.7500	0.1900	0.2217	0.1759	0.8241	Predicted oil zone	150	11,400
	Well-029	0.4444	0.4145	0.2296	0.2963	0.7037	Predicted oil zone	100	11,400
	Well-048	0.6296	0.2915	0.2796	0.3792	0.6208	Predicted oil zone	150	10,750
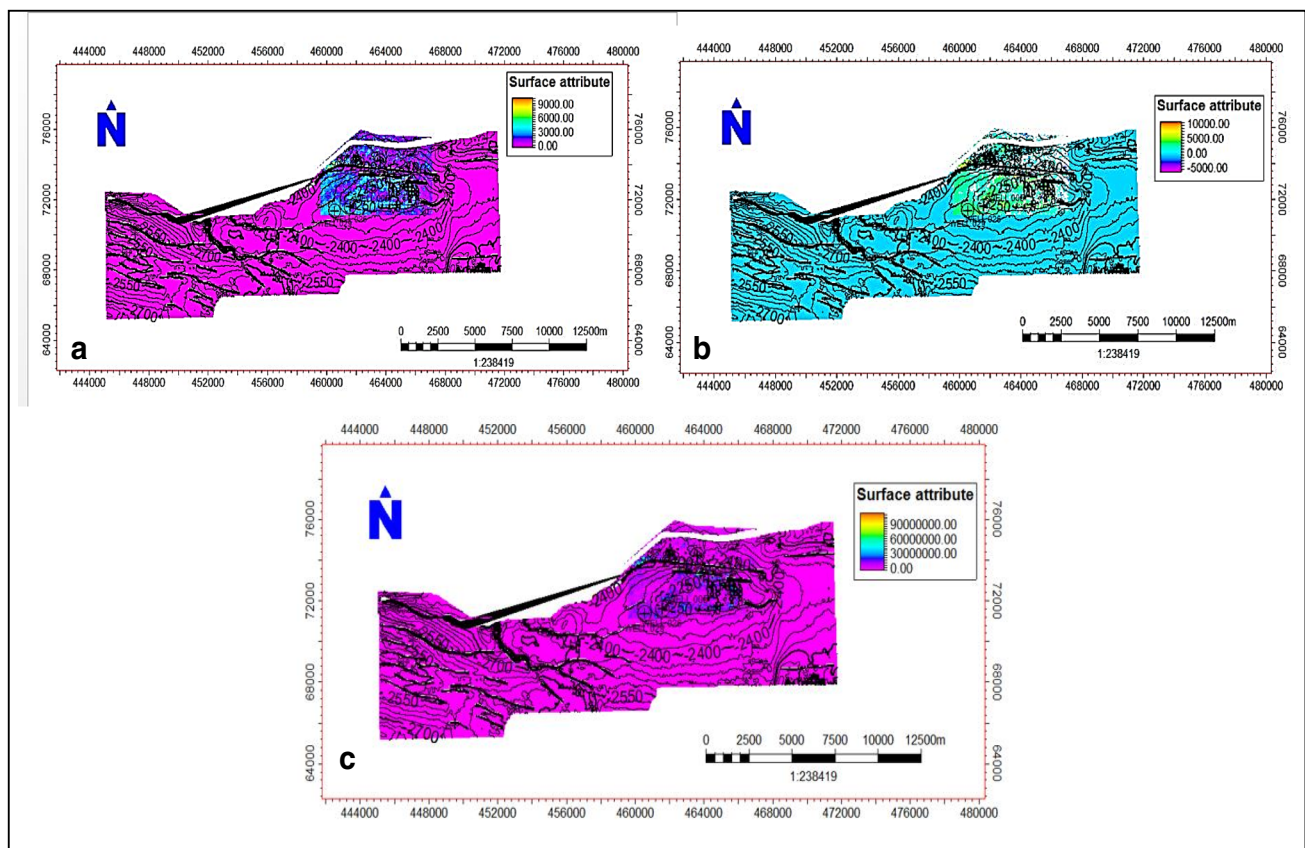
Fig. 8 Surface attribute maps of the F-1000 reservoir indicating areas of probable hydrocarbon accumulation. **a** Root mean square (RMS) amplitude attribute map showing the closure low range values. **b** Maximum amplitude attribute map showing the closure high range values. **c** Average energy attribute map showing the closure low range values

gross or possible hydrocarbon compartments of low economic quantity. However, the noticeable anticlines and fault-assisted closures within the study area suggest good trapping mechanism and hydrocarbon prospects in the Niger Delta (Weber and Daukoru 1975; Alao et al. 2013). Furthermore, the progradational stacking patterns of the gamma ray log (Fig. 6b) suggests rapid filling of the accommodation space than it is created, resulting in facies progressively moving
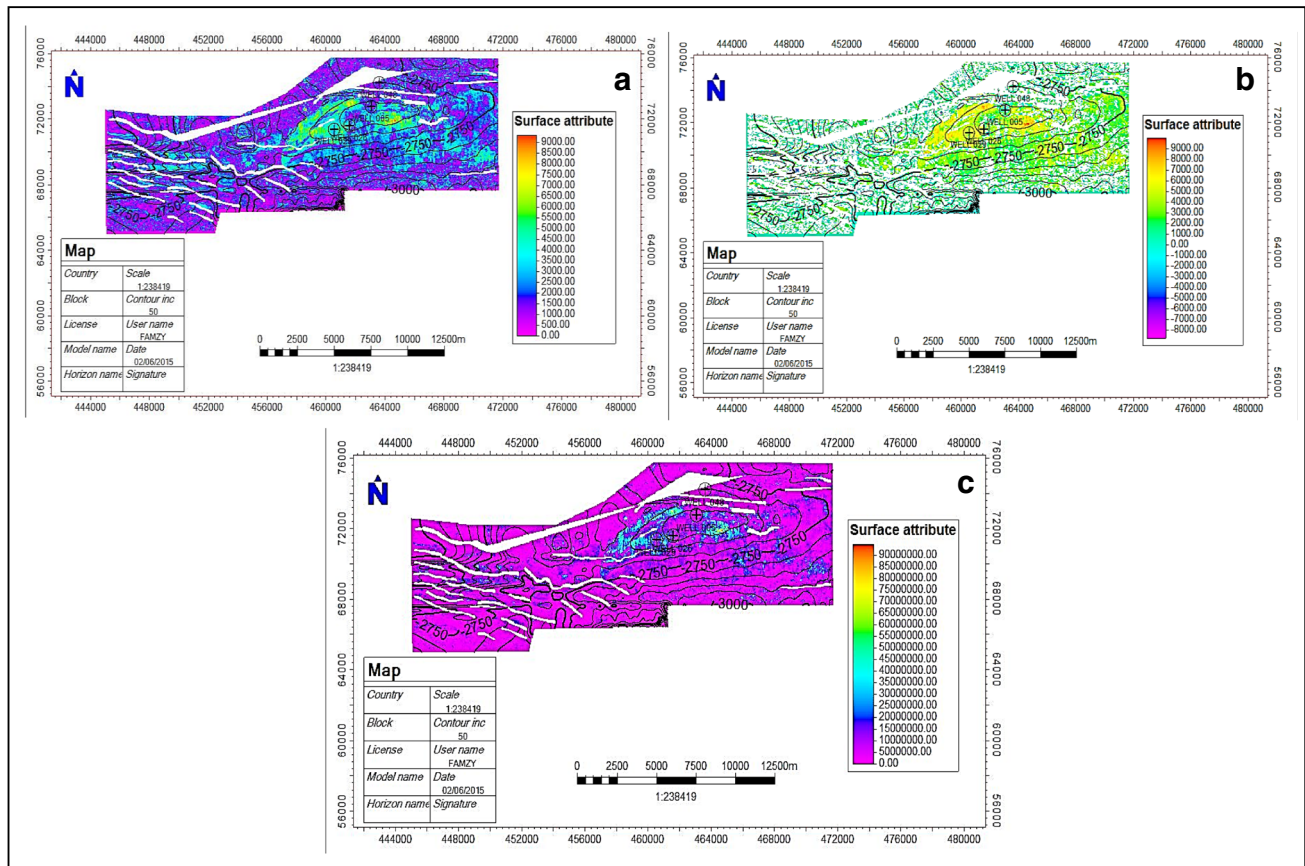
Fig. 9 Surface attribute maps of the G-1000 reservoir indicating areas of probable hydrocarbon accumulation. **a** Root mean square (RMS) amplitude attribute map showing the closure low range values. **b** Maximum amplitude attribute map showing the closure high range values. **c** Average energy attribute map showing the closure low range values

farther seawards over time and building out to form coarsening upward sequences (Catuneanu et al. 2011). On the other hand, the retrogradational stacking pattern indicates more accommodation (water depth becomes deeper) than fluvial inputs, causing facies to progressively move farther landwards (Catuneanu et al. 2011). Similar observations have been reported in the work of Neal and Abreu (2009), where the concept of accommodation succession stacking was used in the interpretation of stratigraphic data within a hierarchal framework of depositional sequences, sequence sets, and composite sequences.

The generally low values of average energy and moderate to high values of RMS and maximum amplitude surface attributes suggest that the wells drilled across the field targeted compartments made up of sand-rich sediments (Figs. 8, 9, and 10). This provides a good guide for enhanced assessment of the overall reservoir structure and prediction of potential hydrocarbon charged areas that are away from the drilled locations. G-1000 and H-1000 reservoirs reveal structures away from the main closure that is amplitude supported. This could be linked to slightly compacted sand

deposits showing fairly strong hydrocarbon build at the western part of the field. This is likely considering the work of Alao et al. (2013) who predicted such prospective hydrocarbon zones in the Niger Delta to have good porosity, permeability, and hydrocarbon saturation from surface attribute analysis, and the work of Emujakporue and Enyenihi (2020), which attempted to classify hydrocarbon presence in Akos field reservoir by utilizing surface attributes such as RMS, amplitude envelope, and instantaneous frequency.

Conclusion

This study evaluates the hydrocarbon prospectivity of three reservoirs (F-1000, G-1000, and H-1000) in the Famito field, Coastal Swamp Niger Delta, using an integrated seismic and well log dataset. The interpretations of the results generated from these dataset show that:

- Ten major and several minor faults were mapped, which trend in a dominantly E-W direction and dip to the south,
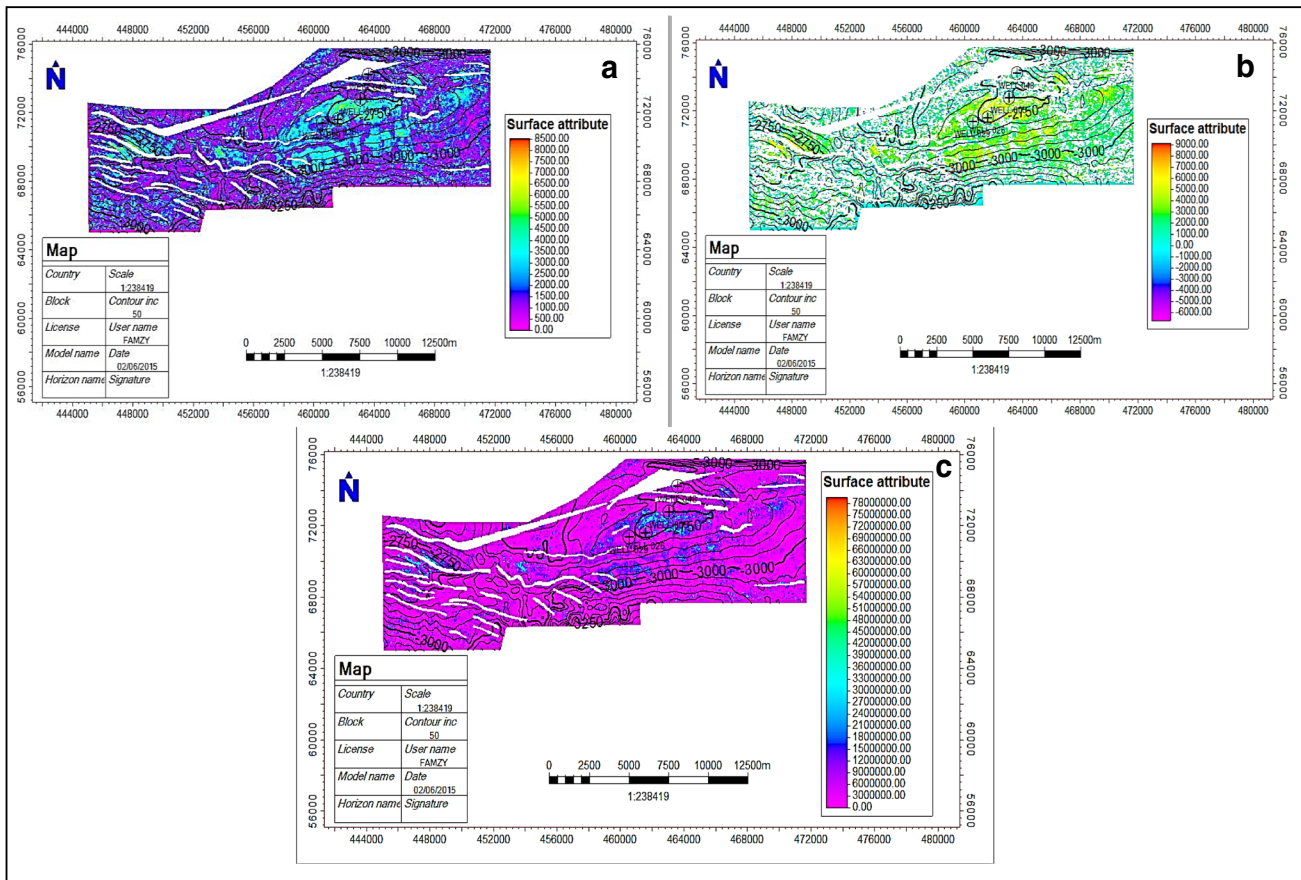
Fig. 10 Surface attribute maps of the H-1000 reservoir indicating areas of probable hydrocarbon accumulation. **a** Root mean square (RMS) amplitude attribute map showing the closure low range val-ues. **b** Maximum amplitude attribute map showing the closure high range values. **c** Average energy attribute map showing the closure low range values

interpreted as syn-sedimentary deformation resulting from the load of the overlying sediments.

- The three delineated reservoirs are laterally continuous with good sand development down-dip as the delta prograded. Three stacking patterns are identified within the F-1000 reservoir, a progradational stacking pattern, dominant at the base, an aggradational stacking pattern at the middle, and a retrogradational stacking pattern seen at the top section of the reservoir.
- The average petrophysical properties across the three reservoirs show good to excellent values that range between 19 and 30% volume of shale, 24 and 25% porosity, and 61 and 72% hydrocarbon saturation.
- Surface attribute analysis shows that hydrocarbon presence is closely tied to strong amplitude on attribute maps extracted along the horizon and suggests that the most prospective region is the north-eastern part of the field area.
- Ultimately, new prospect compartments have been advised for hydrocarbon volume assessment and drill-

ing to optimize production within the field. The discovery of these new prospective areas indicates the effectiveness of surface attributes in identifying new pay zones within active fields, which can be applied in the Eocene to Holocene sequence of other petroleum provinces.

Author contribution CAI and CCU conceptualized the project. JNE and COE participated in data curation, formal analysis, data interpretation, and manuscript drafting.

Declarations

Conflict of interest The authors declare that they have no competing interests.

References

Aigbedion I, Aigbedion HO (2011) Hydrocarbon volumetric analysis using seismic and borehole data over 'Umoru' Field, Niger Delta Nigeria. Int J Geosci 2:179–183

Alao PA, Olabode SO, Opeloye SA (2013) Integration of seismic and petrophysics to characterize reservoirs in ALA oil field, Niger Delta. Sci World J 2013:1–15

Amigun JO, Bakare NO (2013) Reservoir evaluation of "Danna" field Niger Delta using petrophysical analysis and 3-D seismic interpretation. Pet Coal 55:119–127

Anene NO, Ehinola OA, Eyinla DS (2018) Sub-surface mapping and reservoir evaluation of "Enena" field, offshore Niger Delta. J Appl Geol Geophys 6:65–73

An P, Moon WM (1993) Reservoir characterization using feedforward neural networks. SEG Technical Program Expanded Abstracts, 258–262

Asquith G, Krygowski D (2004) Basic well log analysis. Am Assoc Pet Geol Methods Explorat Ser 16:52–62

Cant DJ (1992) Subsurface facies analysis. In R.G. Walker and N.P. James (eds.), Facies models: response to sea level changes. St. John's, Newfoundland, Geological Association of Canada.

Catuneanu O, Galloway WE, Kendall CG, Miall AD, Posamentier HW, Strasser A, Tucker ME (2011) Sequence stratigraphy: methodology and nomenclature. News Lett Strat 44:173–245

Corredor F, Shaw JH, Bilotti F (2005) Structural styles in the deepwater fold and thrust belts of the Niger Delta. Am Assoc Pet Geol Bull 89:753–780

Dim CIP, Onuoha KM, Anyiam OA, Okwara IC, Oha IA, Okonkwo IA, Ozumba BM (2018) Analysis of petroleum system for exploration and risk reduction in the southeastern inland basins of Nigeria. Pet Coal 60:305–320

Doust H, Omatsola E (1990) Niger Delta. In: J. D. Edwards, and P.A. Santogrossi, (eds.), Divergent/ passive margin basins. Am Assoc Pet Geol 48:239–248

Ehinola OA, Ejeh OI (2009) Basin geometry and sedimentary fill modeling of parts of onshore Niger Delta, Nigeria. Kuwait J Sci Engrg 36:147–163

Ehinola OA, Shengfei Q, Onibonoje AA (2010) Paleoenvironmental significance of pyritic nodules from Lokpanta oil shale interval in the petroleum system of lower Benue Trough, Nigeria. Pet Coal 52:110–122

El Sharawy M, Nabawy B (2016) Geological and petrophysical characterization of the Lower Senonian Matulla Formation in Southern and Central Gulf of Suez. Egypt Arab J Sci Eng 41:281–300

Emujakporue GO, Enyenihi EE (2020) Identification of seismic attributes for hydrocarbon prospecting of Akos field, Niger Delta, Nigeria. SN Appl Sci 2:1–11

Eshimokhai S, Akhirevbulu OE (2012) Reservoir characterization using seismic and well logs data (a case study of Niger Delta). Ethiop J Environ Stud Manag 5:597–603

Evamy BD, Haremboure J, Kamerling P, Knaap WA, Molloy FA, Rowlands PH (1978) Hydrocarbon habitat of Tertiary Niger Delta. Am Assoc Pet Geol Bull 62:1–39

Glover P (2013) Petrophysics: M.Sc. Course notes. Quebec, Canada, University of Laval, pp 108–110

Horsfall OI, Davies DH, Davies OA (2015) Hydrocarbon reservoir characterization using well log in Niger Delta basin of Nigeria. Int J Appl Nat Sci 4:55–64

Klett TR, Ahlbrandt TA, Schmoker JW, Dolton GL (1997) Ranking of the world's oil and gas provinces by known petroleum volumes. USGS Open File Report 7–463

Knox GJ, Omatsola EM (1989) Development of the Cenozoic Niger Delta in terms of the escalator regression model and impact on hydrocarbon distribution. In J. Van Der Mascle, M. Marhino, and J. Wanesson (eds.), The structure of the Guinean continental margin: implications for the connections between the Central and South Atlantic Oceans, Geologische Rundschau 75:57–70

Lehner P, De Ruiter PAC (1977) Structural history of Atlantic Margin of Africa. Am Asso Petrol Geol Bull 61:961–981

Opara AI (2010) Prospectivity evaluation of "Usso" Field, onshore Niger Delta Basin, using 3-D seismic and well log data. Pet Coal 52:307–315

Peacock DCP, Knipe RJ, Sanderson DJ (2000) Glossary of normal faults. J Struct Geol 22:291–305

Pochat S, Van Den D, Besnard K, Gumiaux C (2004) A simple method of determining sand/shale ratios from seismic analysis of growth faults: an example from upper Oligocene to lower Miocene Niger Delta deposits. Assoc Pet Geol Bull 88:1357–1367

Nabawy B, El Sharawy M (2015) Hydrocarbon potential, structural setting and depositional environments of Hammam Faraun member of the Belayim Formation, Southern Gulf of Suez. Egypt J Afr Earth Sci 112:93–110

Neal J, Abreu V (2009) Sequence stratigraphy hierarchy and the accommodation succession method. Geology 37:779–782

Radwan A, Nabawy B, Kassem A, Hussein W (2021) Implementation of rock typing on waterflooding process during secondary recovery in oil reservoirs: a case study, El Morgan oil field, Gulf of Suez. Egypt Nat Res Res 30:1667–1696

Reijers TJA (2011) Stratigraphy and sedimentology of the Niger Delta. Geologos 17:133–162

Saadu YK, Nwankwo CN (2018) Petrophysical evaluation and volumetric estimation within central swamp depobelt, Niger Delta, using 3-D seismic and well logs. Egypt J Pet 27:531–539

Selley RC (1998) Elements of petroleum geology. Gulf Professional Publishing, New York

Stacher P (1995) Present understanding of the Niger Delta hydrocarbon habitat. In M.N. Oti and G. Postma, (eds.), Geology of Deltas, Rotterdam, 257–267

Tuttle WLM, Brownfield EM, Charpentier RR (1999) The Niger Delta Petroleum System. Chapter A: Tertiary Niger Delta (Akata-Agbada) Petroleum System, Niger Delta Province, Nigeria, Cameroon and Equatorial Guinea, Africa. U.S. Geological Survey, Open File Report 99–50-H.

Ugbor CC, Emedo CO, Arinze IJ (2020) Interpretation of airborne magnetic and geo-electric data: resource potential and basement morphology of the Ikom-Mamfe embayment and environs, southeastern Nigeria. Nat Resour Res 30:153–174

Unukogbon NO, Asuen GO, Emofurieta WO (2008) Sequence stratigraphic appraisal: coastal swamp depobelt in the Niger Delta Basin Nigeria. Global J Geol Sci 6:129–137

Weber KJ, Daukoru EM (1975) Petroleum geology of the Niger Delta. Proc Ninth World Pet Congr 2:210–221

Wiener RW, Michael GM, Michael TA, Joseph BM (2010) Mobile shale in the Niger Delta: characteristics, structure, and evolution. In L. Wood (ed). Shale tectonics, AAPG Memoir, 93:145 – 161

Whiteman AJ (1982) Nigeria: its petroleum geology, resources and potential. Graham and Trotman, London